Astrocytes Secrete Exosomes Enriched with Proapoptotic Ceramide and Prostate Apoptosis Response 4 (PAR-4)
POTENTIAL MECHANISM OF APOPTOSIS INDUCTION IN ALZHEIMER DISEASE (AD)*[S]

Guanghu Wang[‡1], **Michael Dinkins**[‡1], **Qian He**[‡], **Gu Zhu**[‡], **Christophe Poirier**[§], **Andrew Campbell**[¶], **Margot Mayer-Proschel**[¶], and **Erhard Bieberich**[‡2]

From the [‡]Program in Developmental Neurobiology, Institute of Molecular Medicine and Genetics, Medical College of Georgia, Georgia Health Sciences University, Augusta, Georgia 30912, the [§]Vascular Biology Center, Georgia Health Sciences University, Augusta, Georgia 30912, and the [¶]Department of Biomedical Genetics, University of Rochester Medical Center, University of Rochester, Rochester, New York 14642

Background: In AD, amyloid protein is associated with neurodegeneration, which may involve amyloid effects on astrocytes.
Results: In astrocytes, amyloid peptide triggers secretion of proapoptotic exosomes ("apoxosomes") that are associated with ceramide and PAR-4.
Conclusion: Activation of nSMase2 and expression of PAR-4 is critical for the secretion of apoxosomes and glial apoptosis.
Significance: Apoxosomes may contribute to glial apoptosis, and therefore, neurodegeneration in AD.

Amyloid protein is well known to induce neuronal cell death, whereas only little is known about its effect on astrocytes. We found that amyloid peptides activated caspase 3 and induced apoptosis in primary cultured astrocytes, which was prevented by caspase 3 inhibition. Apoptosis was also prevented by shRNA-mediated down-regulation of PAR-4, a protein sensitizing cells to the sphingolipid ceramide. Consistent with a potentially proapoptotic effect of PAR-4 and ceramide, astrocytes surrounding amyloid plaques in brain sections of the 5xFAD mouse (and Alzheimer disease patient brain) showed caspase 3 activation and were apoptotic when co-expressing PAR-4 and ceramide. Apoptosis was not observed in astrocytes with deficient neutral sphingomyelinase 2 (nSMase2), indicating that ceramide generated by nSMase2 is critical for amyloid-induced apoptosis. Antibodies against PAR-4 and ceramide prevented amyloid-induced apoptosis *in vitro* and *in vivo*, suggesting that apoptosis was mediated by exogenous PAR-4 and ceramide, potentially associated with secreted lipid vesicles. This was confirmed by the analysis of lipid vesicles from conditioned medium showing that amyloid peptide induced the secretion of PAR-4 and C18 ceramide-enriched exosomes. Exosomes were not secreted by nSMase2-deficient astrocytes, indicating that ceramide generated by nSMase2 is critical for exosome secretion. Consistent with the ceramide composition in amyloid-induced exosomes, exogenously added C18 ceramide restored PAR-4-containing exosome secretion in nSMase2-deficient astrocytes. Moreover, isolated PAR-4/ceramide-enriched exosomes were taken up by

astrocytes and induced apoptosis in the absence of amyloid peptide. Taken together, we report a novel mechanism of apoptosis induction by PAR-4/ceramide-enriched exosomes, which may critically contribute to Alzheimer disease.

Alzheimer disease (AD)[3] is a devastating neurodegenerative disease associated with the buildup of protein aggregates within and surrounding neurons in the hippocampus and cortex (1). Two forms of protein aggregates, Tau protein fibrillary tangles and amyloid β (Aβ) protein plaques, are known to induce neuronal malfunction and apoptosis (2). The protein buildup is linked to a variety of mutations, among which mutations of γ-secretase, an enzyme processing the amyloid precursor protein (APP), lead to the most severe forms of AD (3). Aberrant processing of APP results in the secretion, aggregation, and plaque formation of neurotoxic peptides such as the Aβ peptides Aβ1–40, Aβ1–42, and Aβ25–35 (4).

Although most research has focused on the effect of Tau protein tangles and Aβ plaques on neuronal function and survival, it is now well established that astrocytes also play a role in AD pathology (5–14). In the CNS, astrocytes are indispensable for the support of neurons. However, astrocytes can also adopt an activated state where they start to migrate and proliferate and induce inflammatory and proapoptotic cell signaling pathways (8, 10, 15, 16). Astrocytic reactivation has been observed in many neurodegenerative diseases, including AD, and is thought to occur as a response to oxidative stress and cytokine release (8, 10–12, 16–18). As a consequence, astrocytes not only fail to support neurons, but also generate a toxic environment that is detrimental to neurons and astrocytes themselves. Astrocytic

[3] The abbreviations used are: AD, Alzheimer disease; FAD, familial AD; Aβ, amyloid β; APP, amyloid precursor protein; nSMase2, neutral sphingomyelinase 2; GFAP, glial fibrillary acidic protein; Z, benzyloxycarbonyl; FMK, fluoromethyl ketone; UC, ultracentrifugation.

dysfunction combined with cell death has been described to occur in AD; glial apoptosis has been found to be correlated with the number of senile plaques, although a clear association of apoptosis with labeling of Aβ protein has not been shown yet (19). Activation of caspases has been suggested to contribute to astrocyte damage, but the mechanism by which astrocytes might die in AD remains unclear (20).

In this study, we propose a novel mechanism that sensitizes astrocytes to amyloid-induced cell death via concurrent up-regulation of PAR-4 and ceramide. We also demonstrate that the level of proapoptotic ceramide in astrocytes is regulated by neutral sphingomyelinase 2 (nSMase2). Further, we show for the first time that astrocytic apoptosis is associated with the secretion of PAR-4/ceramide-containing lipid vesicles (exosomes) that can induce cell death even in cells not exposed to amyloid protein. Therefore, our finding identifies a novel mechanism of apoptosis induction by exosomes that are secreted by amyloid protein-exposed astrocytes.

EXPERIMENTAL PROCEDURES

Materials—Human brain tissue from AD patients was a generous gift from Dr. David Hill, Georgia Health Sciences University, Augusta, GA. The 5XFAD mouse was purchased from The Jackson Laboratory (Bar Harbor, ME). Amyloid peptides were from AnaSpec (Fremont, CA) and rPeptide (Bogart, GA). Anti-ceramide antibody was generated in our laboratory (rabbit IgG) or obtained from Glycobiotech (mouse IgM; Kuekels, Germany). Anti-PAR-4, PKCζ (atypical PKC), CD9, and anti-GFAP antibodies were from Santa Cruz Biotechnology (Santa Cruz, CA). Monoclonal anti-TSG101 mouse IgG was from Abcam (Cambridge, MA). Monoclonal anti-amyloid 4G8 IgG was obtained from Millipore (Billerica, MA). The anti-activated caspase 3 antibody was obtained from Cell Signaling Technology (Danvers, MA). Fluorophore-conjugated secondary antibodies were from Jackson ImmunoResearch Laboratories (West Grove, PA). Magnetic beads coated with anti-rabbit IgG were obtained from Miltenyi (Auburn, CA) and New England Biolabs (Ipswich, MA). Ceramide was obtained from Avanti Polar Lipids (Alabaster, AL). The ExoQuick exosome purification kit and anti-Alix1 rabbit IgG were from System Biosciences SBI (Mountain View, CA). Vybrant CM-DiI and the Click-iT Cy5 TUNEL assay were purchased from Invitrogen. The ProteoStat amyloid plaque detection kit was from Enzo Life Sciences (Farmingdale, NY). All reagents were of analytical grade or higher.

Cultivation of Primary Astrocytes and Incubation with Amyloid Peptide—Cortical primary astrocytes were prepared from postnatal day 1–3 pups following an established protocol (21). The proportion of astrocytes was quantified by immunocytochemistry using an antibody against GFAP. A typical culture was found to consist of more than 95% of GFAP$^+$ cells. The astrocytes were incubated with amyloid peptide and other reagents in phenol red and serum-free medium. When *fro/fro* pups were used, genotyping was performed twice using tail- and astrocyte-derived DNA following standard protocols. Fibrillary amyloid peptide 25–35 and 1–42 was prepared using a published protocol (4, 22).

Preparation and Characterization of Exosomes—A fraction of exosomes secreted from astrocytes was prepared by ultracentrifugation as previously published (23, 24). In brief, astrocyte-conditioned medium was first centrifuged for 15 min at $1,000 \times g$ to remove cells and large cell debris. The supernatant was then centrifuged for 30 min at $20,000 \times g$, and the resulting supernatant passed through a 0.22-μm filter to remove residual cell debris. Exosomes were then pelleted by ultracentrifugation for 2 h at $150,000 \times g$, and the pellet was resuspended in 100 μl of phosphate-buffered saline (PBS) for exposure to cells, sphingolipidomic analysis, immunoblotting, or magnetic activated cell sorting using anti-ceramide or anti-CD9 antibodies. Highly purified exosomes were also prepared using ExoQuick, a commercially available exosome purification kit (25).

Lipid Analysis—Lipids were extracted from cells and pelleted vesicles using the Folch extraction method with chloroform/methanol (2:1) as previously described (21). Different ceramide species were quantified in the sphingolipidomics (LC-MS/MS) analysis core facility at the Medical University of South Carolina, Charleston, SC (under the supervision of Dr. Jacek Bielawski). The lipid concentration was normalized to protein and lipid phosphate when analyzing organic cell extracts and to lipid phosphate when analyzing vesicle extracts.

RNAi Knockdown of PAR-4—The shRNA was designed using a commercially available program of the manufacturer (Invitrogen). Regions of the 5′-untranslated, coding, and 3′-untranslated region were chosen, and the oligonucleotides were subcloned into the pFUG-GFP vector. Packing of the lentivirus using 293T cells and transduction of astrocytes with the virus followed a standard protocol. The shRNA clone (3-5) with the forward sequence 5′-ctagcctgtgattcactgcgttgtttcaagagaacaacg-cagtgaatcacaggcttt-3′and the reverse sequence 5′-tcgaaagcc-tgtgattcactgcgttgttctctggaaacaacgcagtgaatca-3′ showed successful knockdown of PAR-4 in astrocytes as determined by immunoblotting.

Injection of Amyloid Peptide—Two μg of Aβ25–35 was mixed with 20% of HiLyte Fluor 488-labeled peptide (AnaSpec) and injected into the hippocampus of wild type (C57BL/6) mouse brain (12 days old) with or without adding 1 μg of anti-ceramide or anti-PAR-4 rabbit IgG (5 μl total). Brains were fixed with 4% paraformaldehyde in PBS 48 h after injection for cryosectioning and immunostaining.

Immunocytochemical and Histochemical Analysis—Astrocytes or frozen brain sections were fixed with 4% paraformaldehyde in PBS and then permeabilized by incubation with 0.2% Triton X-100 in PBS for 5 min at room temperature. The immunostaining of fixed cells or brain sections followed procedures described previously (21). Cell nuclei were stained with 2 μg/ml Hoechst 33258 in PBS for 30 min at room temperature. Amyloid plaques were stained with amyloid-specific antibodies, thioflavin S, or ProteoStat following the manufacturers' protocols. Confocal fluorescence microscopy was performed with an LSM 510 confocal scanning microscope. LSM 510 Meta 3.2 software was used for image acquisition from confocal microscopy. Adobe Photoshop CS2 software was used for background reduction, pseudo-colorizing, and overlaying of pseudo-colorized grayscale images. Images obtained with secondary antibody only were used as negative controls representing the
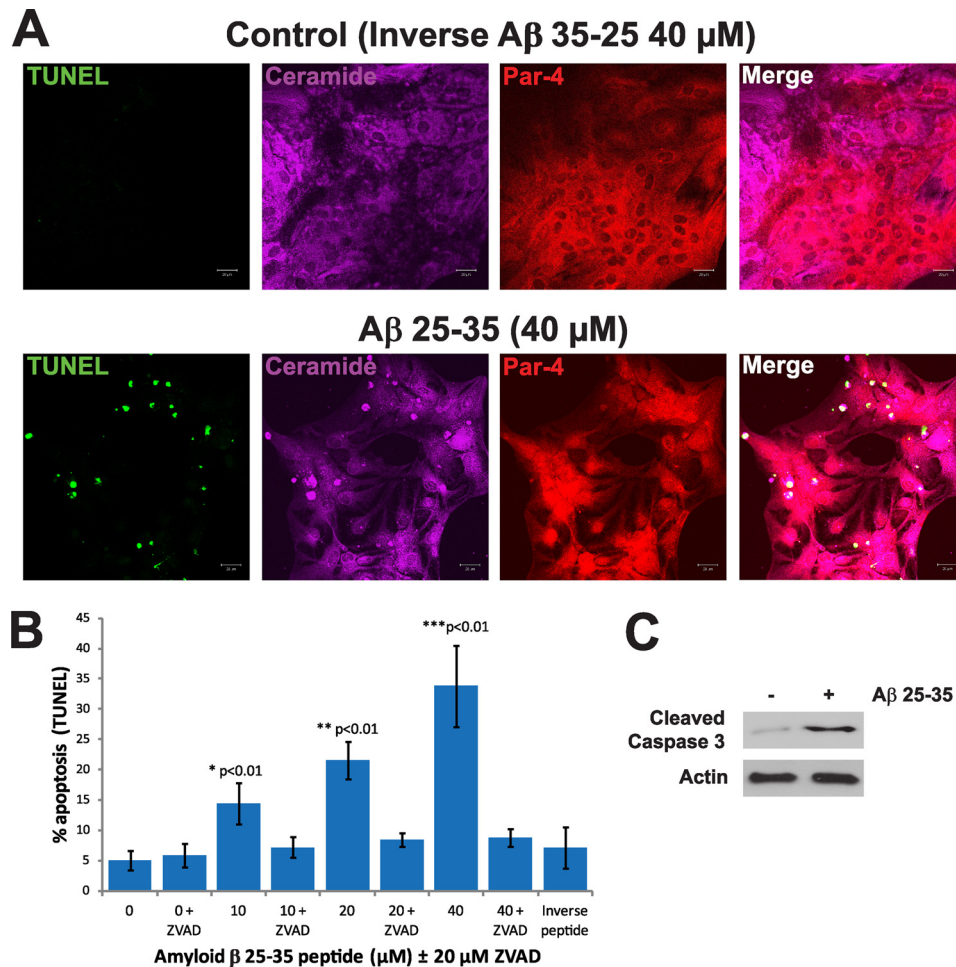
FIGURE 1. **Amyloid peptide induces apoptosis in primary cultures of astrocytes, which is prevented by inhibition of caspases.** *A*, incubation of wild type astrocytes with 40 μM Aβ25–35 or inverse control peptide Aβ35–25 for 24 h. Apoptotic cells were stained with TUNEL. *B*, quantification of apoptotic cells. Note that co-incubation with the cell-permeable pan-caspase inhibitor Z-VAD-FMK prevents Aβ25–35-induced apoptosis. $n = 5$; $p < 0.01$. *, comparison of control (0 μM) with 10 μM Aβ; **, comparison of 10 μM Aβ with 20 μM Aβ; ***, comparison of 20 μM Aβ with 40 μM Aβ. *C*, immunoblotting for cleaved (active) caspase 3 using protein from Aβ25–35-treated and control astrocytes.

background intensity in a particular laser channel. Antigen-specific immunostaining was quantified by counting cells that showed signals 2-fold or more above background fluorescence.

Statistical Analysis—Counting of cells was performed by three individuals in a blinded assay using at least five fields on each section or slide from four independent samples with at least 50 cells in each field. Means and S.D. were determined for counts of single signals, and the two-signal distributions were analyzed using a two-tailed, equal variance Student's *t* test in Microsoft Excel 2007. $p < 0.05$ was considered statistically significant.

RESULTS

Amyloid Peptide Induces Apoptosis in Astrocytes in Vitro through a PAR-4-dependent Mechanism—We performed *in vitro* studies to test whether exposure to the amyloid peptide induced cell death in astrocytes. Primary astrocytes were prepared from the cortex of wild type mice, expanded in serum-containing medium, and then incubated in serum-free medium with various concentrations of the 25–35 and 1–42 amyloid peptides. These two peptide fragments of the amyloid protein are widely used in AD studies and have been shown to induce neuronal apoptosis using a concentration in the 10–50 μM range (26).

Immunocytochemical staining of ceramide and PAR-4 showed that treatment with the amyloid peptides Aβ25–35 and Aβ1–42 induced apoptosis in astrocytes concurrent with the co-expression of PAR-4 and ceramide (Fig. 1*A*, *bottom panel*, see supplemental Figs. S1 and S2 for GFAP immunostaining and phase contrast images). Apoptosis was not detected when the reverse peptide 35–25 was used as the control (Fig. 1*A*, *top panel*, see supplemental Figs. S1 and S2 for GFAP immunostaining and phase contrast images). A quantitative evaluation of TUNEL- or Hoechst-stained (condensed) nuclei showed that 40 μM Aβ25–35 induced apoptosis in more than 30% of the astrocytes (Fig. 1*B*). A similar rate of apoptosis was found for Aβ1–42. Immunoblotting showed that caspase 3 was significantly activated when cells were incubated with Aβ25–35 (Fig. 1*C*). Accordingly, amyloid peptide-induced apoptosis was prevented when astrocytes were incubated with the cell-permeable pan-caspase inhibitor (Z-VAD-FMK) (Fig. 1*B*).

To determine whether expression of PAR-4 was critical for amyloid-induced apoptosis, we knocked down PAR-4 using lentivirus-transduced shRNA. Immunoblotting showed that the shRNA (3-5) reduced the expression of PAR-4 to less than 20% of the wild type level (supplemental Fig. S3A, *lane 4*).
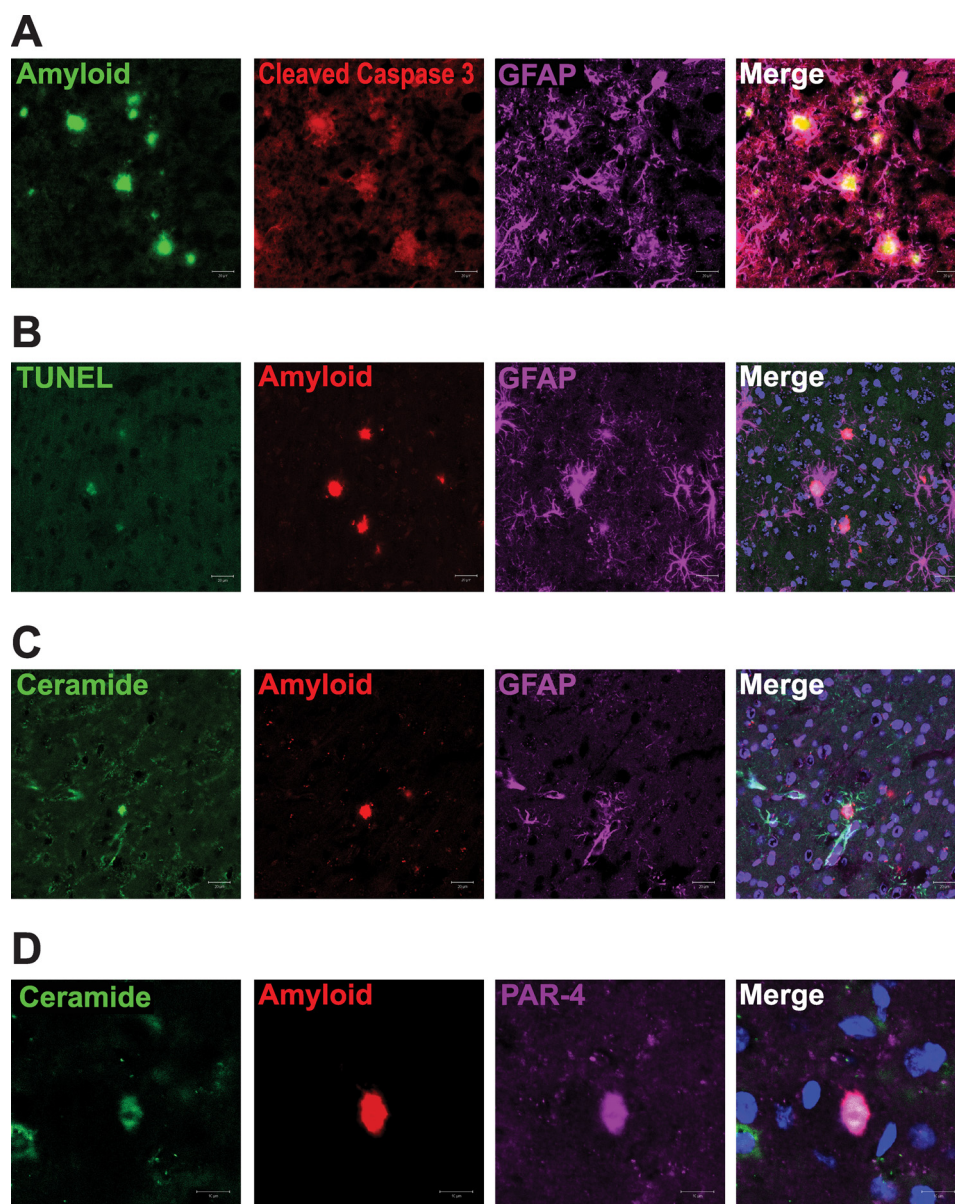
FIGURE 2. **Astrocytes in contact with amyloid co-express ceramide and PAR-4, activate caspase 3, and undergo apoptosis in brain tissue from 5XFAD mouse.** *A–D*, in cryosections of the 5XFAD mouse (8 months of age, cortex), GFAP$^+$ astrocytes that are in contact with amyloid plaques show activation of caspase 3 (*A*, antibody against cleaved caspase 3), undergo apoptosis (*B*), and show co-expression of PAR-4 and ceramide (*C* and *D*).

Down-regulation of PAR-4 was concurrent with up-regulation of Bcl-2, an antiapoptotic protein whose expression is suppressed by PAR-4 (27, 28), which confirmed that the knockdown was specific for PAR-4. Immunocytochemistry for PAR-4 showed that in shRNA-expressing cells (GFP-labeled), the level of amyloid-induced apoptosis (40 μM Aβ25–35) was less than 5% (supplemental Fig. S3*B, bottom panel*). The proportion of apoptotic cells transfected with the lentivirus vector control (30% of the GFP-labeled cells, supplemental Fig. S3*B, top panel*) was comparable with that of amyloid-incubated untransfected cells (Fig. 1*B*). These results confirmed that PAR-4 is a critical factor mediating amyloid-induced apoptosis in astrocytes.

PAR-4 and Ceramide Are Co-expressed in Apoptotic Astrocytes Surrounding Amyloid Plaques—In previous studies, we have shown that ceramide is elevated in hippocampal tissue from newborn presenilin 1 (PS1) knock-in mice, a mouse model for early-onset familial AD (21). A more detailed analysis suggested that ceramide induced apoptosis in PAR-4-expressing astrocytes (21). As our new results showed that PAR-4 was critical for amyloid-induced apoptosis *in vitro*, we tested whether PAR-4 and ceramide were co-expressed in astrocytes *in vivo* by performing immunohistochemical analysis with hippocampal tissue sections derived from the 5XFAD mouse, an AD model with massive amyloid plaque formation, and AD patient brain. The presence of ceramide was confirmed by using two different anti-ceramide antibodies (rabbit IgG and mouse IgM).

Fig. 2*A* shows that in the 5XFAD mouse, GFAP$^+$ cells surrounding amyloid plaques showed activation of caspase 3. About 20% of the plaques were in contact with GFAP$^+$/TUNEL$^+$ cells, indicating that the environment of amyloid plaques induced activation of caspase 3-mediated apoptosis in glial cells (Fig. 2*B*). GFAP$^+$ astrocytes that were not in contact

with amyloid did not show TUNEL labeling, confirming that apoptosis was associated with the presence of plaques. At least 80% of the GFAP$^+$ apoptotic cells were also PAR-4$^+$ and ceramide$^+$, indicating that apoptosis of astrocytes was associated with co-expression of PAR-4 and ceramide (Fig. 2, *C* and *D*, see supplemental Fig. S6*A* for differential interference contrast images). These results were consistent with immunohistochemical analysis of AD patient brain sections (supplemental Fig. S4), suggesting that amyloid induces apoptosis in astrocytes co-expressing PAR-4 and ceramide.

Ceramide Generated by nSMase2 Is Critical for Amyloid Peptide-induced Apoptosis in Astrocytes—We next determined whether inhibition of ceramide generation could prevent amyloid-induced apoptosis in astrocytes. Because it has been suggested recently that the elevation of ceramide by amyloid is triggered by the activation of nSMase2 (29), we exposed primary cultures of astrocytes from the nSMase2-deficient *fro/fro* mouse to Aβ25–35 and determined apoptosis using the TUNEL assay. The *fro/fro* mouse carries a chemically induced deletion within the nSMase2-encoding gene, which leads to reduction of ceramide levels, dwarfism, and early postnatal death (30).

Fig. 3*A* shows that the number of TUNEL$^+$ cells was significantly reduced in Aβ25–35-treated nSMase2-deficient astrocytes when compared with their wild type littermates (see also supplemental Fig. S5 for phase contrast images). This was confirmed by a quantitative analysis with several cultures of astrocytes from different *fro/fro* mice (Fig. 3*B*). Interestingly, apoptosis was not completely prevented in these cells, suggesting that activation of nSMase2 is a major, but not sole, mechanism by which amyloid peptide triggers apoptosis in astrocytes.

Because previous studies showed that there are pro- and nonapoptotic ceramide species (21), we then determined the effect of amyloid peptide on the elevation of particular ceramide species in astrocytes. Ceramide was recovered from control or Aβ25–35-treated wild type or nSMase2-deficient (*fro/fro*) astrocytes by organic solvent extraction and then quantified using sphingolipidomic analysis. Fig. 3*C* shows that amyloid peptide exposure was associated with the elevation of the three major ceramide species, C16, C18, and C24:1 ceramide, in wild type astrocytes. In particular, C18 ceramide was significantly elevated by amyloid peptide. In *fro/fro* astrocytes, the overall ceramide content was reduced by 50% and not elevated by amyloid peptide exposure (Fig. 3*C*). These results suggested that distinct ceramide species generated by nSMase2-catalyzed hydrolysis of sphingomyelin may play a critical role in amyloid peptide-induced apoptosis.

nSMase2 Mediates Amyloid-induced Secretion of PAR-4-associated Exosomes—We next determined the mechanism by which PAR-4 and ceramide facilitated induction of apoptosis. Several clues came from previous studies showing that nSMase2 is critical for the secretion of lipid vesicles termed exosomes and that secreted PAR-4 induced apoptosis in prostate cancer cells (31, 32). Based on these studies and our results, we hypothesized that amyloid peptide-induced activation of nSMase2 triggers ceramide-enriched lipid vesicle formation and secretion of PAR-4, potentially with these two proapoptotic factors physically associated in secreted lipid vesicles.
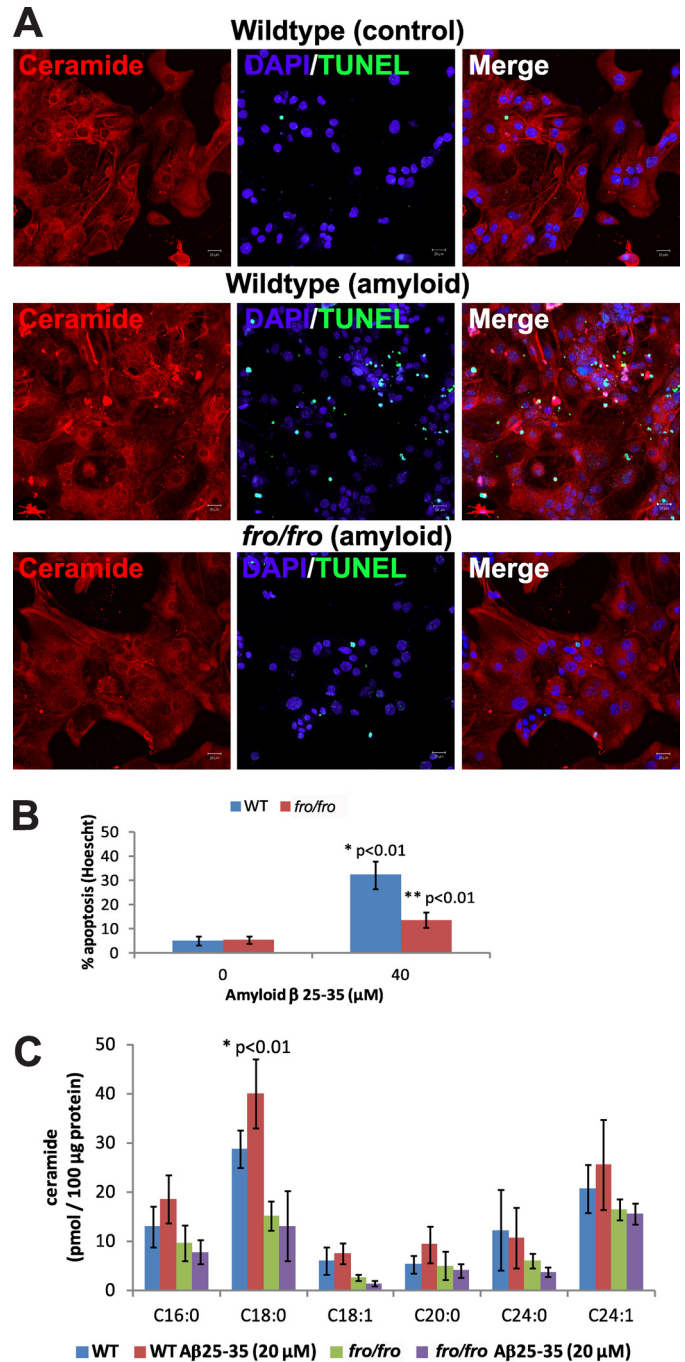

FIGURE 3. **nSMase2-deficient astrocytes from *fro/fro* mouse are protected from amyloid peptide-induced apoptosis and do not show elevation of ceramide.** *A*, primary astrocytes from wild type or homozygous *fro/fro* pups (siblings) were cultivated and incubated with Aβ25–35. Note that there are significantly fewer TUNEL$^+$ cells in *fro/fro* astrocytes. *B*, quantification of *A*. $n = 5$; $p < 0.01$. *, comparison of WT control with WT Aβ-treated cells; **, comparison of WT Aβ with *fro/fro* Aβ. *C*, lipids were extracted with organic solvent from control or Aβ25–35-treated wild type or *fro/fro* astrocytes, and the individual ceramide species were quantified by mass spectrometry using sphingolipidomic analysis. Note that incubation with amyloid peptide leads to the elevation of several ceramide species in wild type, but not in nSMase2-deficient astrocytes. Total ceramide is reduced by half in these astrocytes. $n = 3$; $p < 0.05$.

We incubated wild type or *fro/fro* astrocytes for 48–72 h with 20–40 μM Aβ25–35 in serum-free medium and subjected the medium supernatant to a differential centrifugation protocol and another precipitation method yielding highly purified exo-
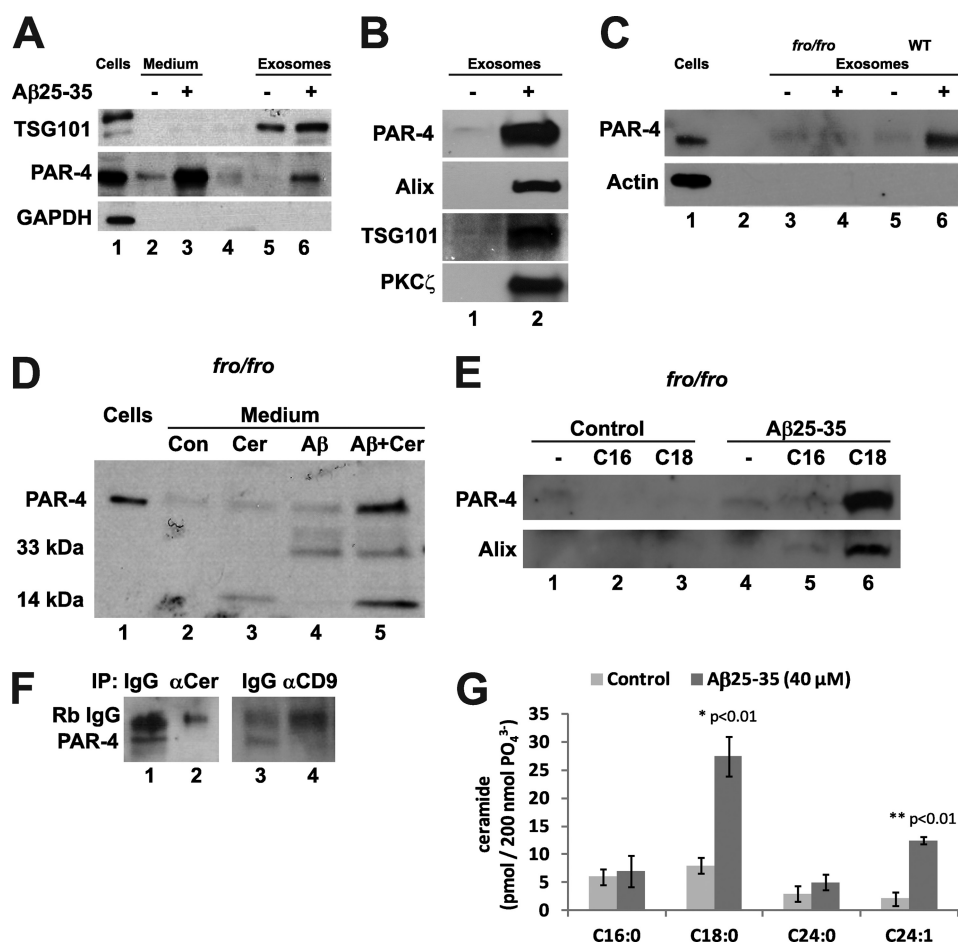
FIGURE 4. **Amyloid peptide triggers secretion of PAR-4 and ceramide in lipid vesicles that induce apoptosis in astrocytes.** *A*, wild type astrocytes were incubated with 20 μM Aβ25–35 for 48 h in serum-free medium, and secreted vesicles were harvested from the medium by ultracentrifugation (UC). *Lane 1*, cell lysate; *lane 2*, medium control (Aβ35–25); *lane 3*, Aβ25–35-treated astrocytes; *lane 4*, marker proteins (not stained); *lane 5*, UC pellet from control astrocytes; *lane 6*, Aβ-treated astrocytes. *B*, exosomes harvested by centrifugation with the ExoQuick reagent. *Lane 1*, control (Aβ35–25); *lane 2*, Aβ25–35-treated astrocytes. *Alix*, Alix1. *C*, UC pellets from wild type and nSMase2-deficient *fro/fro* astrocytes. *Lane 1*, cell lysate; *lane 2*, marker proteins (not stained); *lane 3*, Aβ35–25-treated *fro/fro* astrocytes; *lane 4*, Aβ25–35-treated *fro/fro*; *lanes 5* and *6*, UC pellets from wild type astrocytes. *D*, medium from *fro/fro* astrocytes treated with C16 and C18 ceramide (*Cer*) with or without Aβ25–35. *Lane 1*, cell lysate; *lane 2*, control: *lane 3*, C16 + C18 ceramide; *lane 4*, amyloid peptide; *lane 5*, amyloid peptide + ceramide. *E*, as described for *D*, but exosomes were isolated using ExoQuick reagent and a combination of Aβ25–35 with either C16 (*lane 5*) or C18 ceramide (*lane 6*). *F*, co-immunoprecipitation (*IP*) assay using lipid vesicles resuspended from the UC pellet of medium conditioned by Aβ25–35-treated wild type astrocytes. Vesicles were subjected to magnetic activated cell sorting, and the flow-through fraction was analyzed by immunoblotting. *G*, sphingolipidomic analysis of lipid vesicles in the UC pellet wild type astrocytes without or with Aβ25–35 incubation. $n = 2$; $p < 0.05$ (*); $p < 0.01$ (**).

somes, ExoQuick, to harvest exosomes released to the medium (24, 25). Fig. 4*A* shows that PAR-4 was enriched in the medium when wild type astrocytes were incubated with Aβ25–35 (*lane 3*). There were only trace amounts of PAR-4 in the medium from astrocytes treated with the inactive inverse peptide Aβ35–25 used as the control (*lane 2*), suggesting that the elevation of PAR-4 in the medium was due to the incubation with the active amyloid peptide. The absence of staining for GAPDH confirmed that PAR-4 was not passively released to the medium from dying cells or cell debris, but actively secreted. This was consistent with the observation that PAR-4 was recovered from an ultracentrifugation pellet, which also contained the exosome marker protein TSG101 (*lane 6*). A more specific isolation method using the ExoQuick system demonstrated that PAR-4 was associated with exosomes, which was confirmed by staining for the exosome markers TSG101 and Alix1 (Fig. 4*B*). The observation that the amount of TSG101 or Alix1 was concurrently increased with that of PAR-4 suggested that amyloid peptide elevated the amount of PAR-4-associated exo-

somes. Consistent with this assumption, the exosome fraction contained atypical PKC, a protein kinase we have shown to form a complex with ceramide and PAR-4 (33–36). In contrast to wild type cells, astrocytes cultivated from nSMase2-deficient *fro/fro* brain did not secrete PAR-4 or ceramide when exposed to Aβ25–35 (Fig. 4*C*, *lanes 3* and *4*). These results suggested that nSMase2 was instrumental for the amyloid peptide-induced secretion of PAR-4-associated exosomes.

Next, we tested whether ceramide was critical for the secretion of exosomal PAR-4 from amyloid peptide-exposed astrocytes. *fro/fro* astrocytes were treated with an equimolar mixture of exogenous C16 and C18 ceramide (2 μM each), 40 μM Aβ25–35, or a combination of ceramide and amyloid peptide. These two ceramide species were chosen because they were elevated by amyloid peptide (Fig. 3*C*). They have also been shown to be taken up by cells when added to the medium (34, 37–43). Fig. 4*D* shows that incubation with ceramide or Aβ25–35 moderately elevated secretion of proteins that were stained for PAR-4, but of lower molecular masses (33 or 14 kDa). However, when
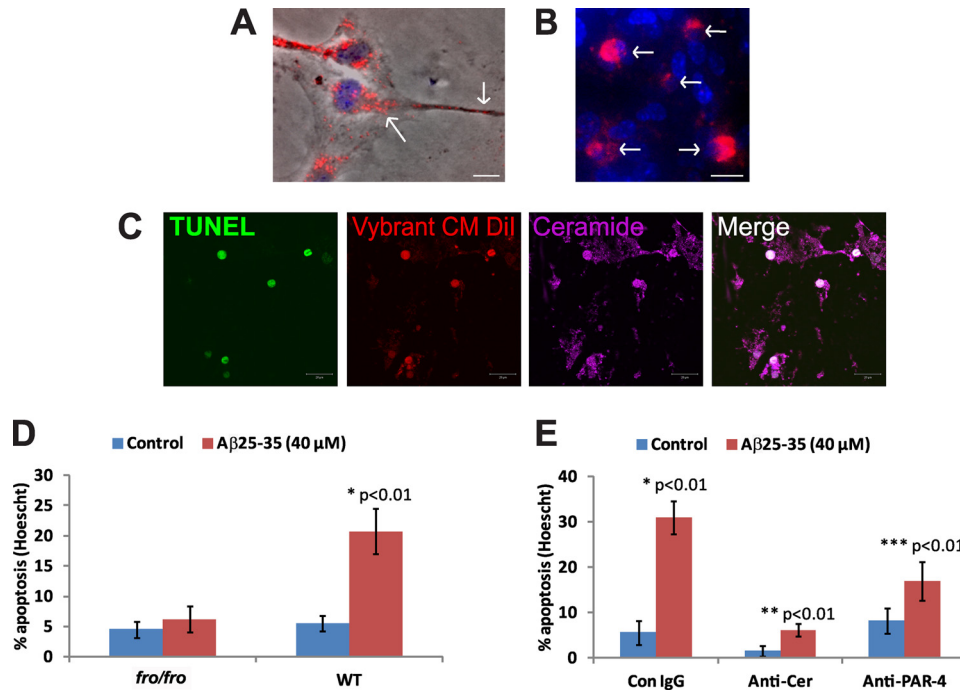
FIGURE 5. **Exosomes isolated from medium of amyloid peptide-treated astrocytes induce apoptosis.** Wild type astrocytes were loaded with Vybrant CM-DiI and then incubated with fresh medium supplemented with 20 μM Aβ25–35. *A*, red fluorescence is visible in a perinuclear compartment and vesicles along processes and at the cell membrane (*arrows*). *Bar* = 5 μm. *B*, exosomes were resuspended and added to wild type astrocytes. Only astrocytes taking up exosomes (*red fluorescent, arrows*) round up and show condensed nuclei (Hoechst dye, *blue*). *Bar* = 10 μm. *C*, confocal laser scanning immunofluorescence microcopy of exosome-treated astrocytes using TUNEL staining and anti-ceramide rabbit IgG (Cy5, pseudo-colored in *blue*). *Bar* = 20 μm. *D*, quantification of apoptosis induced by exosomes from Aβ25–35-treated wild type astrocytes. $n = 3, p < 0.01$. *E*, quantification of apoptosis induced by Aβ25–35 in the presence of anti-ceramide (*Anti-Cer*) or PAR-4 IgG (1 μg/ml). $n = 5; p < 0.01$. *Con*, control. *, comparison control IgG with amyloid-treated control IgG; **, comparison anti ceramide IgG with amyloid-treated anti ceramide IgG; ***, comparison anti PAR-4 IgG with amyloid-treated anti PAR-4 IgG.

combined, exogenous ceramide and amyloid peptide dramatically increased secretion of full-length PAR-4 (Fig. 4*D, lane 5*), which was associated with exosomes (Fig. 4*E, lanes 5* and *6*). Interestingly, when combined with Aβ25–35, C18 ceramide was >4-fold more potent in triggering the secretion of PAR-4-associated exosomes (Fig. 4*E, lane 6*) than C16 ceramide (*lane 5*, see supplemental Fig. S5 for phase contrast images). This result was consistent with the observation that C18 ceramide was most elevated in amyloid peptide-treated wild type astrocytes (Fig. 3*C*) and suggested that this particular ceramide species was critical for the amyloid-induced secretion of exosomes and their association with PAR-4.

PAR-4-associated Exosomes Are Enriched with C18 and C24:1 Ceramide—To determine whether ceramide was specifically enriched in PAR-4-associated exosomes, we further analyzed the vesicular pellet obtained by ultracentrifugation of the medium from control and amyloid peptide-treated astrocytes. We incubated medium-derived vesicles from Aβ25–35-treated wild type astrocytes with magnetic beads that were coated with anti-ceramide rabbit IgG, anti-CD9 rabbit IgG, or nonspecific control IgG. The beads were then removed using magnetic activated cell sorting, and the flow-through was analyzed for the presence of PAR-4. Fig. 4*F* shows that anti-ceramide IgG and anti-CD9 IgG, but not control IgG, depleted the vesicle fraction of PAR-4, suggesting that PAR-4 is associated with ceramide-containing vesicles secreted to the medium. The presence of CD9 confirmed that the PAR-4/ceramide-containing vesicles were exosomes, consistent with the results of the ExoQuick purification procedure (Fig. 4*B*).

We then analyzed the exosomes for their content of ceramide. A mass spectrometric (sphingolipidomics) analysis showed that the lipid vesicles from Aβ25–35-treated astrocytes were enriched with C18 and C24:1 ceramide and that C18 ceramide was the predominant ceramide species (Fig. 4*G*). This result was consistent with the observation that amyloid peptide induced elevation of this ceramide species in wild type astrocytes (Fig. 3*C*), concurrent with increased secretion of exosomes (Fig. 4*B*). It was also consistent with the result that exogenous C18 ceramide could specifically restore the secretion of PAR-4-associated exosomes in amyloid peptide-treated *fro/fro* astrocytes (Fig. 4*E*), and therefore, provided further evidence for the assumption that this ceramide species is instrumental for the secretion of exosomes that are associated with PAR-4.

PAR-4/Ceramide Exosomes Induce Apoptosis in the Absence of Amyloid Peptide—So far, we have shown that amyloid peptide induced secretion of exosomes associated with PAR-4 and ceramide. We next tested whether PAR-4/ceramide-containing exosomes induced apoptosis when astrocytes were exposed to them in the absence of amyloid peptide. To detect astrocytes that bound and took up exosomes, we labeled exosomes fluorescently by loading *fro/fro* or wild type astrocytes with Vybrant CM-DiI. This red fluorescent dye is taken up by living cells and permanently stains cellular membranes. We then washed off excess dye in the medium and incubated cells with 20 μM Aβ25–35 or Aβ1–42. After 36 h of incubation, Vybrant CM-DiI was clearly visible in a perinuclear compartment and vesicles in processes and at the cell surface (Fig. 5*A, arrows*, see supplemental Fig. S6*C* for single channel images).

The medium from the Vybrant CM-DiI-loaded and amyloid-treated astrocytes was harvested, and exosomes were isolated by ultracentrifugation. The exosomes were resuspended and then added to wild type astrocytes in the absence of amyloid peptide. Fig. 5*B* shows that astrocytes, which bound and took up exosomes (*red fluorescent, arrows*), rounded up and showed condensed nuclei (*blue, arrows*), two typical characteristics of apoptosis (see supplemental Fig. S6*D* for single channel images and phase contrast). Apoptosis was confirmed using TUNEL staining (Fig. 5*C*). Apoptotic cells that have taken up exosomes strongly stained for ceramide, suggesting that ceramide was supplied to the cells via exosomes, or alternatively, that these vesicles triggered a process of endogenous ceramide generation, ultimately leading to apoptosis. A quantitative analysis confirmed that only the resuspended pellet from medium derived from wild type astrocytes treated with amyloid peptide, but not from wild type astrocytes without amyloid or *fro/fro* astrocytes with or without amyloid, induced apoptosis (Fig. 5*D*). Taken together these results suggested that amyloid peptide triggers the co-distribution and secretion of PAR-4 and ceramide in exosomes that induce apoptosis in astrocytes.

Evidence that the generation and secretion of ceramide-enriched exosomes is a critical step in the induction of apoptosis was obtained by treating cells with antibodies against ceramide. It has been shown that an anti-ceramide antibody prevented cell death induced by extracellular ceramide in lung emphysema, although this previous study did not investigate whether ceramide was presented in the form of lipid vesicles or exosomes (44). Consistent with these results, anti-ceramide IgG, but not nonspecific rabbit IgG used as a control, significantly reduced Aβ25–35-induced apoptosis by blocking extracellular ceramide (Fig. 5*E*). In addition, our results confirmed that ceramide-enriched exosomes are critical for the induction of apoptosis by amyloid peptide. A PAR-4 antibody was only partially effective in preventing apoptosis, suggesting that exosomes enclosing PAR-4 rather than PAR-4 presented at the vesicle surface were responsible for the induction of apoptosis.

The protective effects of anti-ceramide and anti-PAR-4 antibodies were also tested *in vivo* by injecting fluorescently labeled Aβ25–35 into mouse brain, with or without adding anti-ceramide or anti-PAR-4 IgG. TUNEL assays and immunohistochemical analysis for GFAP showed that the addition of the antibodies prevented glial apoptosis induced by the injected amyloid peptide (Fig. 6). Consistent with the assumption that amyloid protein or peptide leads to activation of caspase 3 and eventually induces apoptosis of astrocytes, many apoptotic cells were found within the population of reactive astrocytes migrating toward the lesion site containing the amyloid peptide (Fig. 6*A, arrows*). Used as the control, the contralateral site did not show glial activation or apoptotic cells (Fig. 6*B*). Co-injection of amyloid peptide with anti-ceramide or anti-PAR-4 antibodies prevented glial apoptosis, although migration of reactive astrocytes to the lesion site was still observed (Fig. 6, *C* and *D*). These results were consistent with the *in vitro* data (Fig. 5*E*) and suggested that also *in vivo*, glial apoptosis is induced by amyloid peptide, which is mediated by exogenous ceramide and PAR-4, potentially associated with exosomes.
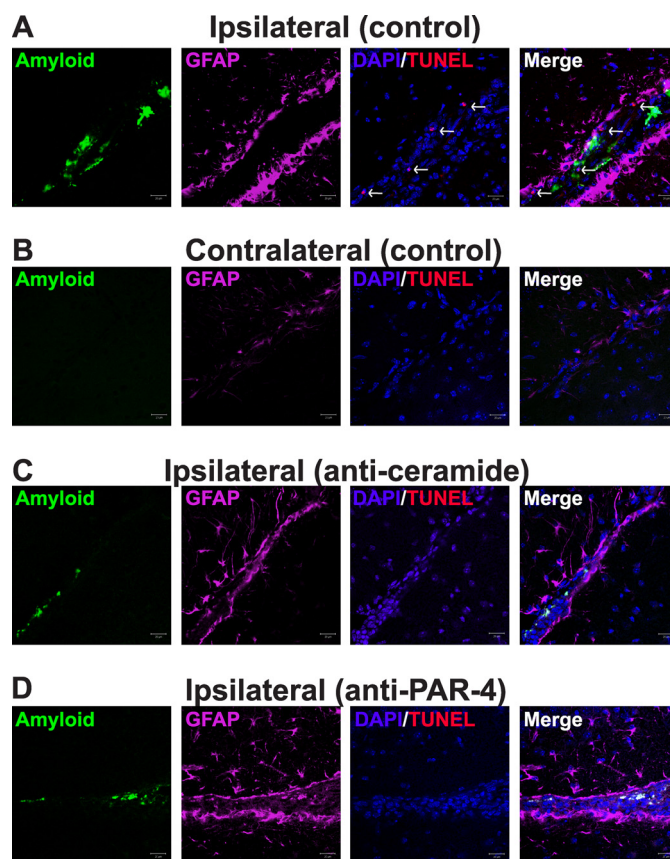

FIGURE 6. **Injection of amyloid peptide into mouse brain induces apoptosis in hippocampal astrocytes, which is prevented by anti-ceramide or anti-PAR-4 antibodies.** Coronal cryosections and confocal immunofluorescence microscopy using an antibody against GFAP (Cy5) and a Cy3 Click-iT TUNEL assay (*arrows* point at apoptotic cells) show that apoptosis is detectable in ~5% of Hoechst-stained cells in the hippocampus in an area of 100 μm surrounding the injected amyloid peptide. About 70% of these cells are GFAP$^+$ (*n* = 2). There are no TUNEL$^+$ cells detectable when anti-ceramide or anti-PAR-4 antibodies are co-injected with the amyloid peptide. *A*, Aβ-injected; ipsilateral; *B*, Aβ-injected, contralateral; *C*, anti-ceramide antibody-co-injected, ipsilateral; *D*, anti-PAR-4 antibody-co-injected, ipsilateral.

Finally, to test whether PAR-4 and ceramide were co-distributed with exosomes in cells, we performed immunocytochemistry for PAR-4, ceramide, and TSG101 in control and amyloid peptide-treated astrocytes. In control astrocytes, immunostaining of PAR-4, ceramide, and TSG101 showed only little overlap (Fig. 7*A*). Upon treatment with amyloid peptide, PAR-4, ceramide, and TSG101 were redistributed to the perinuclear region and to numerous vesicles in processes (Fig. 7*B*, see supplemental Fig. S6*B* for phase contrast images). At higher magnification (Fig. 7*C*), co-distribution at the cell surface of astrocytic processes appeared in vesicle- or bleb-like structures similar to the structures stained with Vybrant CM-DiI (Fig. 5*A*). When astrocytes were treated with Vybrant CM-DiI-labeled exosomes, attached vesicles were co-localized with ceramide (Fig. 7*D* and fluorescence profile in Fig. 7*E*), suggesting that astrocytic processes are sites for the dynamic exchange of ceramide- and PAR-4-associated exosomes.

DISCUSSION

The present study reveals a novel mechanism by which ceramide- and PAR-4-enriched exosomes can induce apoptosis in
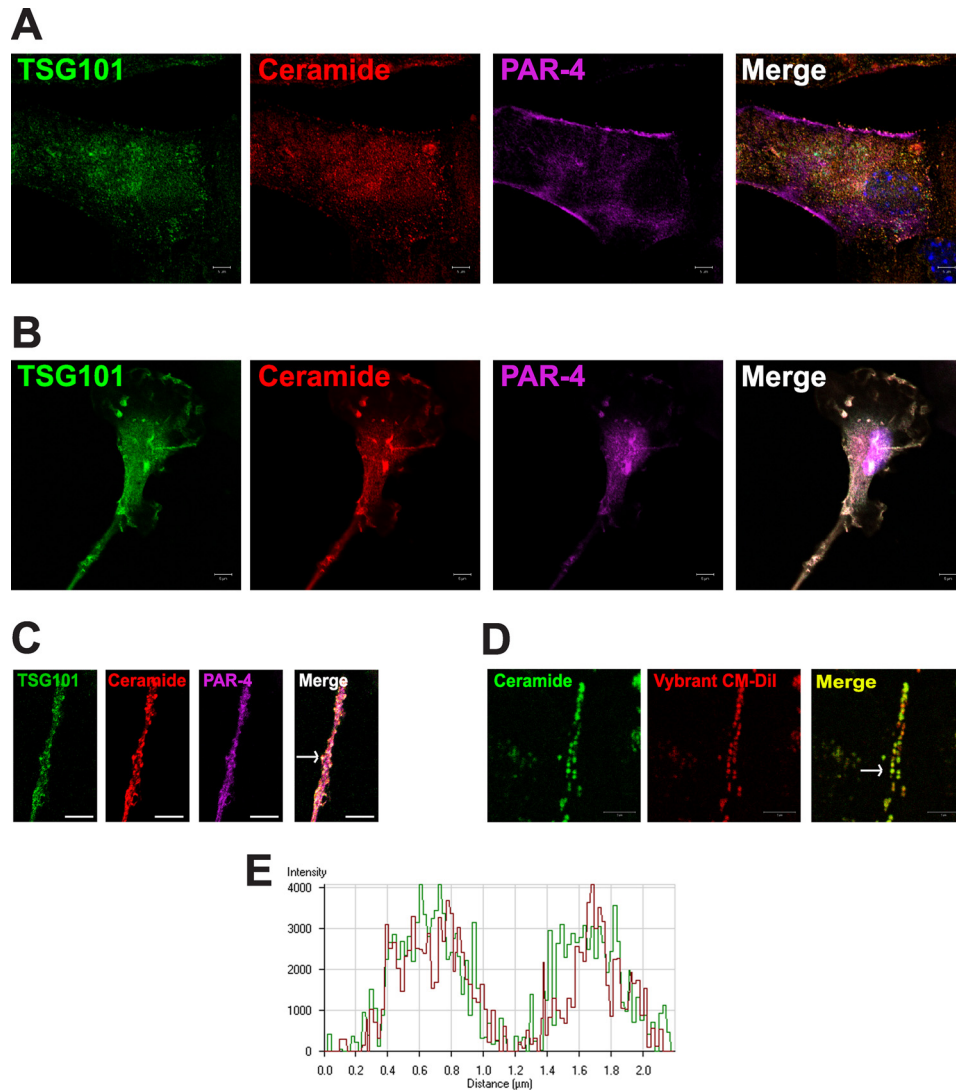
FIGURE 7. **PAR-4 and ceramide are associated with exosomes secreted by amyloid peptide-treated astrocytes.** *A*, control cells not treated with amyloid do not show co-distribution of PAR-4, ceramide, and TSG101. *Bar* = 2 μm. *B*, Aβ25–35 treatment induces co-distribution of PAR-4, ceramide, and TSG101, which is predominantly found in the perinuclear region and bleb-like membrane structures on the surface of astrocytic processes (*arrow*). *Bar* = 1 μm. *C–E*, incubation of astrocytes with Vybrant CM-DiI-labeled exosomes shows co-distribution with TSG101, ceramide, and PAR-4 (profile analysis of pixel intensity in *E*). *Bar* = 3 μm.

astrocytes and potentially other cell types. Given the role of these exosomes in apoptosis, we propose that they will be referred to as *apoxosomes*. Further, our results strongly suggest that nSMase2 is critical for the enrichment of ceramide in apoxosomes. Ceramide may contribute to apoxosome formation and secretion or induction of apoptosis in astrocytes when presented in the form of apoxosomes.

We previously showed that the expression of PAR-4 and the simultaneous elevation of ceramide induce apoptosis in neural progenitor cells (45, 46). Ceramide is a sphingolipid that is generated by the sphingomyelinase-catalyzed hydrolysis of sphingomyelin and is known to induce apoptosis in cells that are sensitive to it. We have shown that elevation of PAR-4 sensitizes neural progenitor cells toward ceramide (33, 45–47). Further, we found that long chain ceramide induces apoptosis in astrocytes from the Psen1 AD mouse, whereas wild type astrocytes appear to be resistant to ceramide (21). We suggested that the ceramide sensitivity of Psen1-derived astrocytes resulted

from the elevated expression of PAR-4, which was not found in wild type astrocytes.

As most AD patients do not carry the *PSEN1* mutation, the effect of amyloid on wild type astrocytes is likely to be of significance for the etiology of AD. Our new results demonstrate that exposure to the amyloid peptide triggers the secretion of PAR-4 in ceramide-associated vesicles from wild type astrocytes. Consistent with our previous studies, ceramide-induced apoptosis in astrocytes was critically dependent on the expression of PAR-4. Moreover, AD patient brain sections and sections from the 5XFAD mouse showed co-expression of PAR-4 and ceramide concurrent with glial apoptosis when in cells coming into contact with amyloid plaques. The fact that glial apoptosis is not frequently reported in AD (although it has been reported in Ref. 19) can be explained by the rapid clearance of apoptotic cells.

Observations in the 5XFAD mouse are particularly interesting in regard to the fact that the knock-in of a transgene with mutations in *PSEN1* and *APP* is Thy1-dependent, and there-

fore, the mutated amyloid protein is only expressed in neurons. Nevertheless, the plaque size is severalfold larger than that of the plaque-generating neurons, suggesting that amyloid byproducts do not immediately self-intoxicate and kill the neurons, but affect other cells as well. This assumption is supported by our data showing that injected amyloid peptide led to acute apoptosis in reactive astrocytes. Thus, the effects of neuron-derived amyloid peptide on astrocytes would lead to glial and neuronal dysfunction, and eventually, neuronal degeneration. The predominant amyloid peptide in human AD is the fragment composed of amino acids 1–42 of APP (4). Within this fragment, a peptide composed of residues 25–35 (Aβ25–35) is considered the toxic peptide inducing apoptosis in AD. Therefore, we performed most of the experiments with Aβ25–35, which induced apoptosis at the same level as the 1–42 peptide.

Our results also suggest that ceramide elevated by amyloid peptide is a key factor in the events observed in our studies. In a previous study, incubation of astrocytes with amyloid peptide showed intracellular elevation of ceramide *in vitro*, although the ceramide species were not identified, and ceramide secretion or glial apoptosis was not reported (29). To our knowledge, we provide for the first time evidence that amyloid-induced ceramide elevation is associated with glial cell death. Our data based on sphingolipidomic analysis show that C18 ceramide is most elevated, consistent with the composition of ceramides secreted in apoxosomes to the medium of amyloid-treated astrocytes. We found that there is a remarkable correlation between the ceramide species affected by nSMase2 deficiency and those secreted to the medium by amyloid-treated wild type astrocytes. The residual apoptosis in nSMase2-deficient astrocytes suggests that a portion of proapoptotic ceramide may have been generated and secreted by an alternative process. Several enzymatic reactions have been described to generate ceramide, and the role of these reactions in the elevation or secretion of ceramide and the induction of apoptosis in astrocytes will be further investigated in our future studies.

Apart from its role in the induction of apoptosis, nSMase2-deficient astrocytes did not secrete apoxosomes, a result in agreement with previous findings showing that ceramide generation by nSMase2 is required for exosome formation (32). Exogenously added C18 ceramide restored the formation and secretion of PAR-4-associated exosomes in amyloid peptide-treated nSMase2-deficient astrocytes. This result is remarkable in that it clearly shows the significance of a particular ceramide species for exosome formation. It is also in accordance with studies from our laboratory as well as other laboratories showing that exogenous C16 or C18 ceramide is taken up by cells and that specific ceramide vesicles bind to PAR-4 via association with atypical PKC (33, 36–39).

Ceramide may have a dual function by triggering apoxosome formation/secretion as well as inducing apoptosis when incorporated into apoxosomes (Fig. 8). When elevated by amyloid-induced activation of nSMase2, ceramide may induce formation of apoxosomes at multivesicular endosomes, or alternatively, facilitate the release of apoxosomes by promoting fusion of multivesicular endosomes with the cell membrane. Because ceramide and PAR-4 are secreted to the extracellular space, their intracellular concentration may not increase, which will prevent
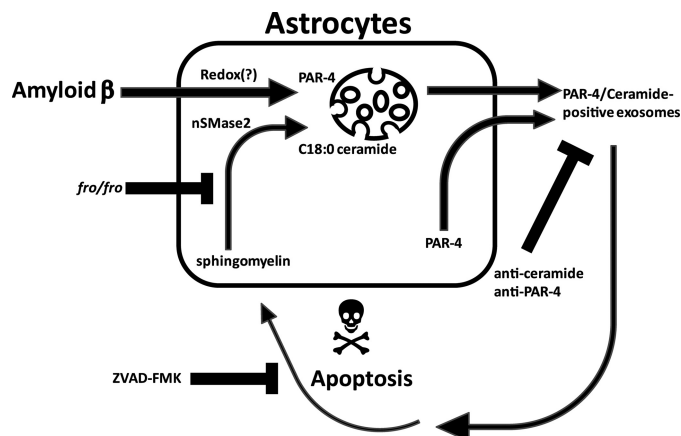

FIGURE 8. **Model for amyloid-induced apoptosis by proapoptotic, PAR-4/ceramide-associated exosomes (apoxosomes).** In astrocytes, contact with amyloid peptide leads to the elevation of ceramide catalyzed by the nSMase2-mediated hydrolysis of sphingomyelin. Ceramide induces exosome formation and association of exosomes with PAR-4. Secreted PAR-4/ceramide-associated exosomes accumulate in the medium until they reach a proapoptotic concentration. Proapoptotic exosomes (apoxosomes) bind to astrocytes and induce apoptosis by the activation of caspase 3. Apoptosis can be prevented by antibodies against ceramide or PAR-4 (neutralizing apoxosomes in the medium) and caspase inhibition (neutralizing apoptosis after binding of apoxosomes).

apoptosis. On the other hand, when accumulating in the medium, apoxosomes may be taken up by astrocytes (*e.g.* by endocytosis) and induce apoptosis. The following lines of evidence strongly suggest that apoxosomes are key factors inducing apoptosis upon incubation of astrocytes with amyloid peptide. 1) Anti-ceramide antibody prevents apoptosis and removes PAR-4 from a lipid vesicle fraction, demonstrating that PAR-4 is physically associated with ceramide vesicles that induce apoptosis. 2) nSMase2-deficient astrocytes do not secrete PAR-4/ceramide-associated apoxosomes and show significantly reduced apoptosis, indicating that nSMase2 is critical for the initial step of amyloid-induced apoxosome secretion. The addition of C18 ceramide to the medium restores apoxosome secretion. 3) Apoxosomes isolated from the medium of amyloid peptide-treated wild type astrocytes induce apoptosis in astrocytes without further addition of amyloid, suggesting that glial apoptosis occurs as a second step in response to the secretion and accumulation of apoxosomes.

In summary, our study shows for the first time that amyloid peptide triggers the secretion of PAR-4 and ceramide from astrocytes. It also shows that PAR-4 and ceramide are associated in apoxosomes, the secretion of which is critically dependent on ceramide release from sphingomyelin by nSMase2. Finally, our results define a mechanism by which amyloid induces apoptosis in astrocytes, which may then significantly contribute to neurodegeneration in AD. Apoxosome secretion by amyloid peptide-exposed astrocytes precedes glial cell death, and therefore, is rather an aberrant process, possibly in self-defense of astrocytes against neurons that generate toxic amyloid fragments. It is also likely that apoxosome secretion is a mechanism to rid astrocytes of proapoptotic PAR-4 and ceramide. In our future studies, we will further investigate the effects of amyloid peptide on astrocytes and the consequences for neurons. In this respect, a recent study by Yuyama *et al.* (48) suggests that neuronal exosomes facilitate clearance of amyloid

peptide by microglia, a function depending on the activation of nSMase2 in neurons. It remains to be investigated whether glial exosomes participate in this process, and therefore, have additional functions distinct from induction of apoptosis. We will also determine whether blocking of ceramide generation or the proapoptotic effect of PAR-4/ceramide-associated apoxosomes is a possible treatment option for AD.

REFERENCES

1. Goedert, M., and Spillantini, M. G. (2006) A century of Alzheimer disease. *Science* **314,** 777–781
2. Ittner, L. M., and Götz, J. (2011) Amyloid-β and Tau: a toxic *pas de deux* in Alzheimer disease. *Nat. Rev. Neurosci.* **12,** 65–72
3. Czech, C., Tremp, G., and Pradier, L. (2000) Presenilins and Alzheimer disease: biological functions and pathogenic mechanisms. *Prog. Neurobiol.* **60,** 363–384
4. Millucci, L., Ghezzi, L., Bernardini, G., and Santucci, A. (2010) Conformations and biological activities of amyloid-β peptide 25–35. *Curr. Protein Pept. Sci.* **11,** 54–67
5. Verkhratsky, A., Olabarria, M., Noristani, H. N., Yeh, C. Y., and Rodriguez, J. J. (2010) Astrocytes in Alzheimer disease. *Neurotherapeutics* **7,** 399–412
6. Mattson, M. P., Pedersen, W. A., Duan, W., Culmsee, C., and Camandola, S. (1999) Cellular and molecular mechanisms underlying perturbed energy metabolism and neuronal degeneration in Alzheimer and Parkinson diseases. *Ann. N.Y. Acad. Sci.* **893,** 154–175
7. Perez, J. L., Carrero, I., Gonzalo, P., Arevalo-Serrano, J., Sanz-Anquela, J. M., Ortega, J., Rodriguez, M., and Gonzalo-Ruiz, A. (2010) Soluble oligomeric forms of β-amyloid (Aβ) peptide stimulate Aβ production via astrogliosis in the rat brain. *Exp. Neurol.* **223,** 410–421
8. Agostinho, P., Cunha, R. A., and Oliveira, C. (2010) Neuroinflammation, oxidative stress, and the pathogenesis of Alzheimer disease. *Curr. Pharm. Des.* **16,** 2766–2778
9. Farfara, D., Lifshitz, V., and Frenkel, D. (2008) Neuroprotective and neurotoxic properties of glial cells in the pathogenesis of Alzheimer disease. *J. Cell Mol. Med.* **12,** 762–780
10. Li, C., Zhao, R., Gao, K., Wei, Z., Yin, M. Y., Lau, L. T., Chui, D., and Hoi Yu, A. C. (2011) Astrocytes: implications for neuroinflammatory pathogenesis of Alzheimer disease. *Curr. Alzheimer Res.* **8,** 67–80
11. Rodríguez, J. J., Olabarria, M., Chvatal, A., and Verkhratsky, A. (2009) Astroglia in dementia and Alzheimer disease. *Cell Death Differ.* **16,** 378–385
12. Meda, L., Baron, P., and Scarlato, G. (2001) Glial activation in Alzheimer disease: the role of Aβ and its associated proteins. *Neurobiol. Aging* **22,** 885–893
13. Nagele, R. G., Wegiel, J., Venkataraman, V., Imaki, H., Wang, K. C., and Wegiel, J. (2004) Contribution of glial cells to the development of amyloid plaques in Alzheimer disease. *Neurobiol. Aging* **25,** 663–674
14. Allaman, I., Bélanger, M., and Magistretti, P. J. (2011) Astrocyte-neuron metabolic relationships: for better and for worse. *Trends Neurosci.* **34,** 76–87
15. Fuller, S., Steele, M., and Münch, G. (2010) Activated astroglia during chronic inflammation in Alzheimer disease: do they neglect their neuro-supportive roles? *Mutat. Res.* **690,** 40–49
16. Lee, Y. J., Han, S. B., Nam, S. Y., Oh, K. W., and Hong, J. T. (2010) Inflam-

17. Croisier, E., and Graeber, M. B. (2006) Glial degeneration and reactive gliosis in α-synucleinopathies: the emerging concept of primary gliodegeneration. *Acta Neuropathol.* **112,** 517–530
18. Van Eldik, L. J., Thompson, W. L., Ralay Ranaivo, H., Behanna, H. A., and Martin Watterson, D. (2007) Glia proinflammatory cytokine up-regulation as a therapeutic target for neurodegenerative diseases: function-based and target-based discovery approaches. *Int. Rev. Neurobiol.* **82,** 277–296
19. Kobayashi, K., Hayashi, M., Nakano, H., Fukutani, Y., Sasaki, K., Shimazaki, M., and Koshino, Y. (2002) Apoptosis of astrocytes with enhanced lysosomal activity and oligodendrocytes in white matter lesions in Alzheimer disease. *Neuropathol. Appl. Neurobiol.* **28,** 238–251
20. Mouser, P. E., Head, E., Ha, K. H., and Rohn, T. T. (2006) Caspase-mediated cleavage of glial fibrillary acidic protein within degenerating astrocytes of the Alzheimer disease brain. *Am. J. Pathol.* **168,** 936–946
21. Wang, G., Silva, J., Dasgupta, S., and Bieberich, E. (2008) Long-chain ceramide is elevated in presenilin 1 (PS1M146V) mouse brain and induces apoptosis in PS1 astrocytes. *Glia* **56,** 449–456
22. Millucci, L., Raggiaschi, R., Franceschini, D., Terstappen, G., and Santucci, A. (2009) Rapid aggregation and assembly in aqueous solution of Aβ (25–35) peptide. *J. Biosci.* **34,** 293–303
23. Fauré, J., Lachenal, G., Court, M., Hirrlinger, J., Chatellard-Causse, C., Blot, B., Grange, J., Schoehn, G., Goldberg, Y., Boyer, V., Kirchhoff, F., Raposo, G., Garin, J., and Sadoul, R. (2006) Exosomes are released by cultured cortical neurons. *Mol. Cell Neurosci.* **31,** 642–648
24. Guescini, M., Genedani, S., Stocchi, V., and Agnati, L. F. (2010) Astrocytes and glioblastoma cells release exosomes carrying mtDNA. *J. Neural Transm.* **117,** 1–4
25. Taylor, D. D., Zacharias, W., and Gercel-Taylor, C. (2011) Exosome isolation for proteomic analyses and RNA profiling. *Methods Mol. Biol.* **728,** 235–246
26. Caraci, F., Chisari, M., Frasca, G., Canonico, P. L., Battaglia, A., Calafiore, M., Battaglia, G., Bosco, P., Nicoletti, F., Copani, A., and Sortino, M. A. (2005) Nicergoline, a drug used for age-dependent cognitive impairment, protects cultured neurons against β-amyloid toxicity. *Brain Res.* **1047,** 30–37
27. Mattson, M. P., Duan, W., Chan, S. L., and Camandola, S. (1999) Par-4: an emerging pivotal player in neuronal apoptosis and neurodegenerative disorders. *J. Mol. Neurosci.* **13,** 17–30
28. Cheema, S. K., Mishra, S. K., Rangnekar, V. M., Tari, A. M., Kumar, R., and Lopez-Berestein, G. (2003) Par-4 transcriptionally regulates Bcl-2 through a WT1-binding site on the *bcl-2* promoter. *J. Biol. Chem.* **278,** 19995–20005
29. Jana, A., and Pahan, K. (2010) Fibrillar amyloid-β-activated human astroglia kill primary human neurons via neutral sphingomyelinase: implications for Alzheimer disease. *J. Neurosci.* **30,** 12676–12689
30. Aubin, I., Adams, C. P., Opsahl, S., Septier, D., Bishop, C. E., Auge, N., Salvayre, R., Negre-Salvayre, A., Goldberg, M., Guénet, J. L., and Poirier, C. (2005) A deletion in the gene encoding sphingomyelin phosphodiesterase 3 (*Smpd3*) results in osteogenesis and dentinogenesis imperfecta in the mouse. *Nat. Genet.* **37,** 803–805
31. Burikhanov, R., Zhao, Y., Goswami, A., Qiu, S., Schwarze, S. R., and Rangnekar, V. M. (2009) The tumor suppressor Par-4 activates an extrinsic pathway for apoptosis. *Cell* **138,** 377–388
32. Trajkovic, K., Hsu, C., Chiantia, S., Rajendran, L., Wenzel, D., Wieland, F., Schwille, P., Brügger, B., and Simons, M. (2008) Ceramide triggers budding of exosome vesicles into multivesicular endosomes. *Science* **319,** 1244–1247
33. Wang, G., Silva, J., Krishnamurthy, K., Tran, E., Condie, B. G., and Bieberich, E. (2005) Direct binding to ceramide activates protein kinase Cζ before the formation of a proapoptotic complex with PAR-4 in differentiating stem cells. *J. Biol. Chem.* **280,** 26415–26424
34. Wang, G., Krishnamurthy, K., Umapathy, N. S., Verin, A. D., and Bieberich, E. (2009) The carboxyl-terminal domain of atypical protein kinase Cζ binds to ceramide and regulates junction formation in epithelial cells. *J. Biol. Chem.* **284,** 14469–14475
35. Bieberich, E., Kawaguchi, T., and Yu, R. K. (2000) *N*-Acylated serinol is a

novel ceramide mimic inducing apoptosis in neuroblastoma cells. *J. Biol. Chem.* **275,** 177–181

36. Bieberich, E. (2011) Lipid vesicle-mediated affinity chromatography using magnetic activated cell sorting (LIMACS): a novel method to analyze protein-lipid interaction. *J. Vis. Exp.* **26,** pii: 265

37. Gamen, S., Hanson, D. A., Kaspar, A., Naval, J., Krensky, A. M., and Anel, A. (1998) Granulysin-induced apoptosis. I. Involvement of at least two distinct pathways. *J. Immunol.* **161,** 1758–1764

38. Herget, T., Esdar, C., Oehrlein, S. A., Heinrich, M., Schütze, S., Maelicke, A., and van Echten-Deckert, G. (2000) Production of ceramides causes apoptosis during early neural differentiation in vitro. *J. Biol. Chem.* **275,** 30344–30354

39. Paris, F., Grassmé, H., Cremesti, A., Zager, J., Fong, Y., Haimovitz-Friedman, A., Fuks, Z., Gulbins, E., and Kolesnick, R. (2001) Natural ceramide reverses Fas resistance of acid sphingomyelinase$^{-/-}$ hepatocytes. *J. Biol. Chem.* **276,** 8297–8305

40. López-Montero, I., Rodriguez, N., Cribier, S., Pohl, A., Vélez, M., and Devaux, P. F. (2005) Rapid transbilayer movement of ceramides in phospholipid vesicles and in human erythrocytes. *J. Biol. Chem.* **280,** 25811–25819

41. Fukunaga, T., Nagahama, M., Hatsuzawa, K., Tani, K., Yamamoto, A., and Tagaya, M. (2000) Implication of sphingolipid metabolism in the stability of the Golgi apparatus. *J. Cell Sci.* **113,** 3299–3307

42. Wang, G., Krishnamurthy, K., Chiang, Y. W., Dasgupta, S., and Bieberich, E. (2008) Regulation of neural progenitor cell motility by ceramide and potential implications for mouse brain development. *J. Neurochem.* **106,** 718–733

43. Wang, G., Krishnamurthy, K., and Bieberich, E. (2009) Regulation of primary cilia formation by ceramide. *J. Lipid Res.* **50,** 2103–2110

44. Petrache, I., Natarajan, V., Zhen, L., Medler, T. R., Richter, A. T., Cho, C., Hubbard, W. C., Berdyshev, E. V., and Tuder, R. M. (2005) Ceramide up-regulation causes pulmonary cell apoptosis and emphysema-like disease in mice. *Nat. Med.* **11,** 491–498

45. Bieberich, E., MacKinnon, S., Silva, J., Noggle, S., and Condie, B. G. (2003) Regulation of cell death in mitotic neural progenitor cells by asymmetric distribution of prostate apoptosis response 4 (PAR-4) and simultaneous elevation of endogenous ceramide. *J. Cell Biol.* **162,** 469–479

46. Bieberich, E., Silva, J., Wang, G., Krishnamurthy, K., and Condie, B. G. (2004) Selective apoptosis of pluripotent mouse and human stem cells by novel ceramide analogues prevents teratoma formation and enriches for neural precursors in ES cell-derived neural transplants. *J. Cell Biol.* **167,** 723–734

47. Bieberich, E. (2011) There is more to a lipid than just being a fat: sphingolipid-guided differentiation of oligodendroglial lineage from embryonic stem cells. *Neurochem. Res.* **36,** 1601–1611

48. Yuyama, K., Sun, H., Mitsutake, S., and Igarashi, Y. (2012) Sphingolipid-modulated exosome secretion promotes the clearance of amyloid-β by microglia. *J. Biol. Chem.* **287,** 10977–10989